Synthesis, Structure and Binding Properties of Nickel and Copper [14]Cyclidene Complexes with Appended Aza Crown Ethers

Bohdan Korybut-Daszkiewicz,*[a] Joanna Taraszewska,*[b] Katarzyna Zięba,[b] Anna Makal,[c] and Krzysztof Woźniak*[c]

Keywords: Cyclidene complexes / Crown ether compounds / Copper / Nickel / Electrochemistry

Copper(II) and nickel(II) cyclidenes linked with one or two 15-azacrown-5 ethers (**3Ni**, **4Ni** and **4Cu**) as well as similar model morpholine-substituted derivatives (**2Cu**, **2Ni**) have been synthesized and characterized using ESI mass-spectrometry, X-ray diffraction, spectroscopic methods and elemental analysis. Cyclic voltammetry of the copper complexes exhibits two reversible redox couples $Cu^{II/III}$ and $Cu^{II/I}$, whereas the nickel complexes show reversible $Ni^{II/III}$ and irreversible $Ni^{II/I}$ redox processes. Cyclic and differential pulse voltammetry have been used to study interactions of metal cations and amino acids with the above complexes. Na^+ and Li^+ interact weakly with the **3Ni** complex. In the presence of Mg^{2+}, the ligand isomerizes from aldehyde to enolate ion, which interacts strongly with Mg^{2+}. The presence of lysine caused a more pronounced shift of the $Cu^{II/III}$ potential in **4Cu** than did leucyne. This suggests that there are interactions between the NH_3^+ group and the crown ether moiety and between the carboxylic group and the Cu^{III} center of the former guest.

Introduction

Redox-active molecular receptors designed to complex and electrochemically recognize charged and neutral guest species have attracted great attention.[1−4] Compounds possessing such properties consist of a redox-active component and a macrocyclic ligand well suited for the complexation of guest species. The redox center in such systems can easily be switched between its oxidized and reduced forms, thus giving two different states with different charges. Each state is expected to behave differently in the binding process with some substrates. Ferrocene crown ethers[1−6] and ferrocene cryptands[7−11] have been the most extensively studied species. However, such electro-active components as cobaltocene[6] quinone, nitrobenzene, and others have also been used.[4] Plenio et al.[8,9] found that efficient electronic communication between the guest coordinated in the macrocyclic cavity and the redox active unit is crucial for the optimum performance of such molecular devices. Some redox switchable host−guest systems have frequently been proposed as the key components of potential molecular devices and sensors.[12,13]

Azamacrocyclic ligands can stabilize unusual oxidation states of coordinated transition metal ions, making them a promising tool for the construction of supramolecular sensors and switches. Rybak-Akimova et al.[14−16] have synthesized a ditopic molecule consisting of 4-formylbenzo-15-crown-5 and a redox-active tetraazamacrocyclic nickel(II) complex as a receptor for $MeNH_3^+$ and β-$AlaH^+$.[14] They also proposed a ditopic receptor for dicarboxylic acids based on a 15-membered tetraazamacrocyclic (cyclidene)-nickel(II) complex conjugated with two cyclic tetraamines (cyclene),[15] and another for the molecular recognition of diammonium cations based on a cyclidene nickel(II) complex bearing two benzocrown ethers.[16] Bernhardt and Hayes[17] applied benzocrown ethers with appended cobalt cyclam as receptors for alkali cations. Fabbrizzi et al.[18] have synthesized luminescent molecular sensors operating through a metal-center redox couple, combining nickel(II) cyclam-like macrocycles or a copper 14-ane-S4 complex with organic fluorophores (mainly anthracene). Previously,[19] we have studied tetraazamacrocyclic nickel(II) complexes functionalized with benzo-15-crown 5 ethers as receptors for group I and II metal cations.

In this paper we describe the synthesis and characterization of 14-member copper(II) and nickel(II) cyclidenes linked with one or two 15-aza-crown-5 ethers (Scheme 1, complexes **3Ni**, **4Ni** and **4Cu**), as potential receptors for alkali, alkaline-earth metal cations and zwitterionic species such as amino acids. Ligands containing binding sites for

[a] Institute of Organic Chemistry, Polish Academy of Sciences, Kasprzaka 44/52, 01-224 Warszawa, Poland
Fax: (internat.) + 48-22-632-6681
E-mail: bkd@icho.edu.pl
[b] Institute of Physical Chemistry, Polish Academy of Sciences, Kasprzaka 44/52, 01-224 Warszawa, Poland
Fax: (internat.) + 48-22-632-5276
E-mail: jota@ichf.edu.pl
[c] Department of Chemistry, University of Warsaw, Pasteura 1, 02-093 Warszawa, Poland

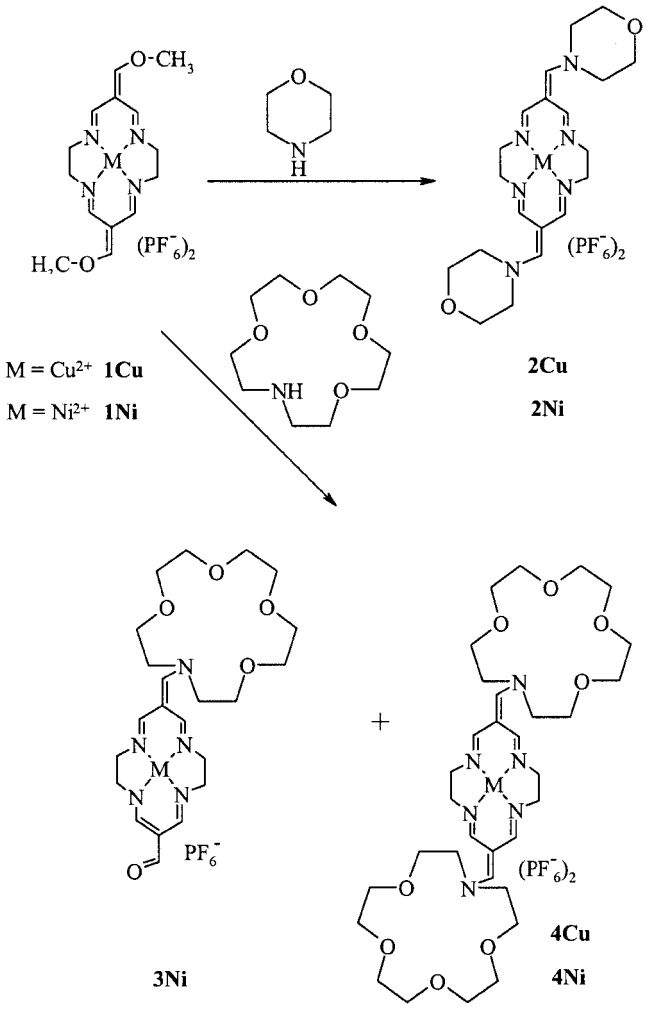

Scheme 1

both cations and anions should be suitable for studying the recognition of such species. This may be important in understanding many biological and communication processes at the molecular level. Transition metal porphyrins[20] and phthalocyanines[21] bearing crown ethers substituents are among several known ditopic macrocyclic molecules containing transition metal and ammonium ion binding sites. Kimura et al.[22] have shown that a molecule composed of a macrocyclic polyamine covalently linked with benzo-15-crown-5 ether forms stable 1:1 complexes with zwitterionic substrates such as amino acids.

Results and Discussion

Synthesis and Structure

Copper(II) and nickel(II) *O*-methylated [14]cylidene complexes **1Cu** and **1Ni** (Scheme 1) reacted with morpholine as well as with 1-aza-15-crown-5 to form amino-substituted cyclidenes **2Cu, 2Ni** or **4Cu, 4Ni**. When complex **1Ni** was used in excess, the monosubstituted product **3Ni** was isolated by chromatography on an SP Sephadex C25 column. Complexes **3Ni** and **4Cu** gave crystals suitable for X-ray analysis.

Structural Details

Complex **4Cu** (Figure 1) crystallizes in the triclinic $P\bar{1}$ space group, as a salt in which two PF_6^- ions interact with one complexed Cu^{II} cation. The complex occupies a special position, with the central Cu atom located exactly on the crystallographic symmetry center. Therefore, the inner symmetry of the molecule becomes a crystallographic feature and, crystallographically, only half of the molecule is independent. Together with one PF_6^- ion the independent half of the **4Cu** molecule defines the crystallographic asymmetric unit.

The macrocyclic fragment of **4Cu** is nearly planar, except for the part including C(1) and C(2), which is an aliphatic part of the ring. The C(1)−C(2) bond length is 1.519 Å and the carbon atoms are above and below the macrocycle plane accordingly. The valence angles C(2)−N(1)−C(3) and C(1)−N(2)−C(5) are close to 120° − a characteristic of such macrocyclic compounds. The bond lengths between other atoms of the macrocyclic moiety reveal their partial double bond character, thus confirming the aromatic character of the tetraazamacrocyclic compound. N(1) and N(2) bind the Cu^{II} cation at the center of the macrocycle with a bond length that is characteristic of N−Cu^{II} interactions (ca. 1.90 Å). C(6) and N(3) are coplanar with the Cu^{II} cation and the coordinating N(1) and N(2) atoms and both C(4)−C(6) and C(6)−N(3) bonds show partial double character, indicating that the lone electron pair of N(3) contributes to the electron density of the aromatic macrocycle. Important bond lengths and angles are given in Table 1. N(3) is nearly coplanar with C(5) and C(3); the rest of the crown ether is forced to be located at close to 100° with respect to the azamacrocyclic moiety. The conformation of the crown ether in this structure is not the most preferable for the coordination of the cations, with the oxygen atoms O(2) and O(4) directed outside the crown and the carbons C(10) and C(15) pointing inwards. Some weak interactions appear to occur between O(1) and O(3) and the hydrogen atoms connected to C(10) and C(15), although the interatomic distances are too long to be classified as regular hydrogen bonds (Table 1). Some reorganization of the crown must occur prior to, or simultaneously with, the process of possible cation complexation. The average C−C and C−O distances in the crown ether are slightly shorter than the average expected C−C and C−O bond lengths (Table 1) but are consistent with the distances reported in crystallographic databases.

The PF_6^- ion shows standard octahedral geometry (Table 1) and is localized close to the macrocycle ring. F(14) interacts with the Cu^{2+} ion (the two atoms are 3.027 Å apart). Together with the macrocyclic nitrogen atoms, F(14) completes the coordination sphere of the Cu^{2+}, making it roughly octahedral, with N(1)−Cu−F(14) and N(2)−Cu−F(14) of 78.92° and 77.68°, respectively. There

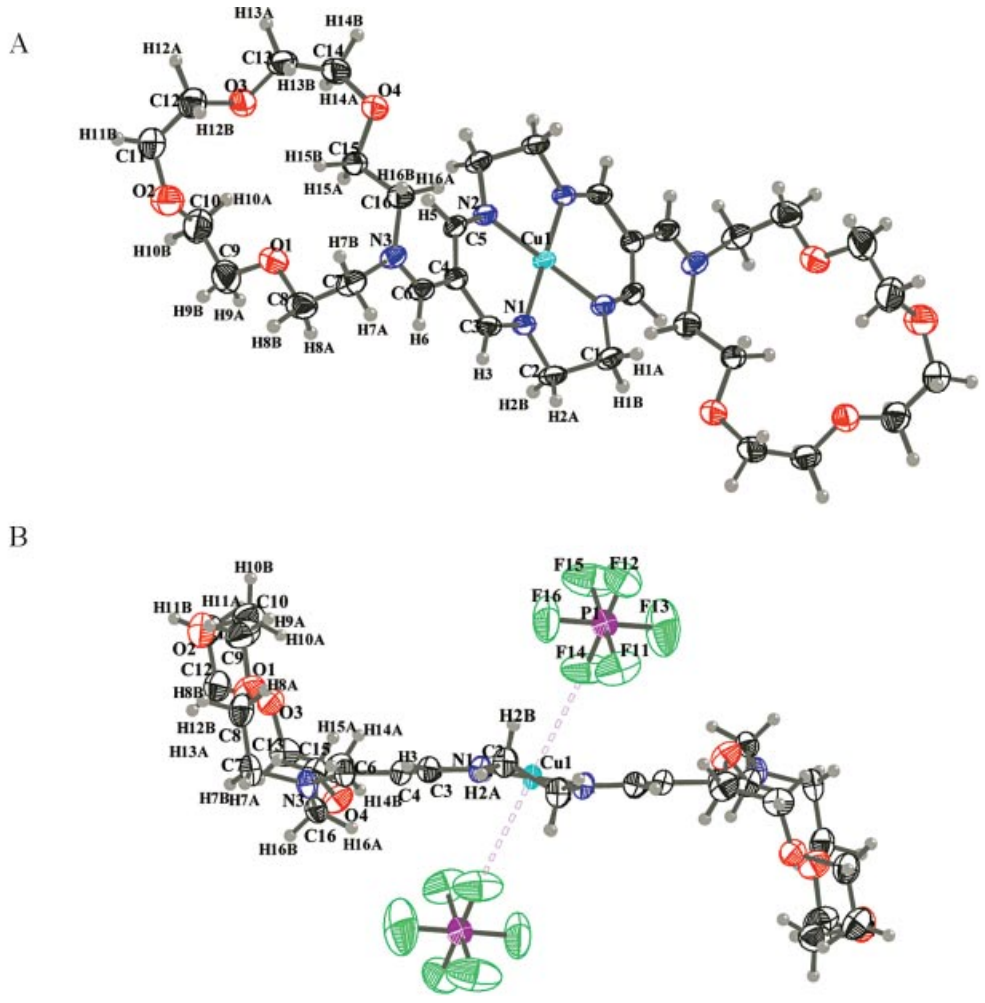

Figure 1. Structure of **4Cu**: (A) with atom labeling, (B) including coordinating PF_6^- molecules

are no other significant interactions between the PF_6^- ion and the macrocyclic Cu complex.

There are also no special intermolecular interactions such as hydrogen bonds that would stabilize the crystal structure of **4Cu**. The packing is rather close and reveals a two-layered structure (Figure 2). The first layer consists of parallel packed macrocyclic moieties and PF_6^- ions while the crown ether compounds build the second layer, forming cages.

3Ni crystallizes in the monoclinic $P2_1/c$ space group, as a salt of one PF_6^- ion interacting with the Ni cation complexed by the macrocyclic compound (Figure 3). The complex occupies a general crystallographic position and together with the PF_6^- ion constitutes the crystallographic asymmetric unit. There are four symmetry related **3Ni** molecules in the unit cell.

The overall structure of the macrocyclic Ni^{II} complex is similar to that in **4Cu**, although there are some differences. The inter-atomic distances between the Ni^{II} ion and the four coordinating nitrogen atoms are slightly shorter than in the **4Cu** structure. This length is characteristic for this type of coordination. The presence of an extra negative charge within the macrocycle ring also has a significant influence. The bonds connecting C(9) with C(8) and C(10)

Table 1. Important structural parameters for **4Cu** (distances in Å)

Parameter definition	
Cu(1)−N(2)	1.913(2)
Cu(1)−N(1)	1.918(2)
C(1)−N(2)#1	1.464(4)
C(1)−C(2)	1.519(4)
C(2)−N(1)	1.465(4)
C(3)−N(1)	1.282(4)
C(3)−C(4)	1.439(4)
C(4)−C(6)	1.399(4)
C(4)−C(5)	1.436(4)
C(5)−N(2)	1.281(4)
C(6)−N(3)	1.313(4)
C(7)−N(3)	1.482(4)
C(16)−N(3)	1.472(4)
Average interatomic distances in the crown ether	
C−C	1.50(3)
C−O	1.41(2)
Average P−F distance	
P−F	1.570(9)

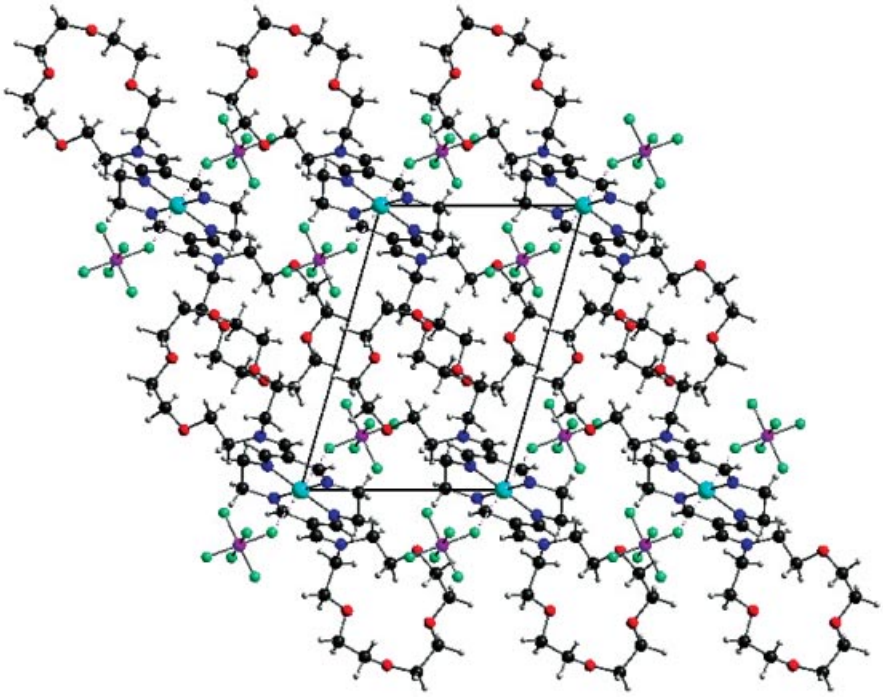

Figure 2. Packing of the **4Cu** molecules in the crystal lattice − view along the *y*-axis

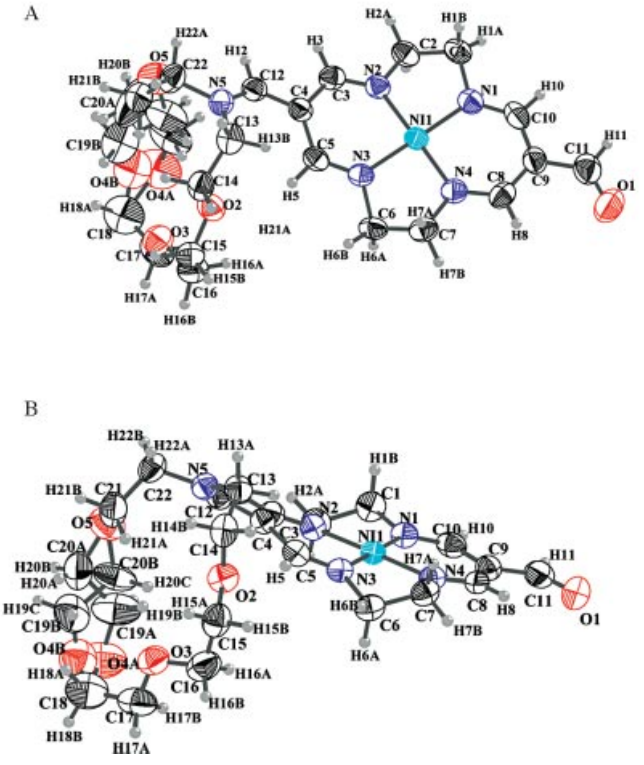

Figure 3. Structure of **3Ni**: (A) view of the macrocyclic compound and (B) presentation of the disorder in the crown ether part

are of equal length and shorter than expected for a typical C−C single bond. This confirms that most of the negative charge is located around C(9), close to the aldehyde group connected with the macrocycle. The exocyclic bond length C(9)−C(11) is typical for a C=C double bond, and the effect is due to both the negative charge on C(9) and the conjugation of the double bond of the carbonyl group with the double bonds of the macrocycle; This is confirmed by the coplanarity of O(1) with C(8) and C(10) (with torsion angles of 1.7° and 179.6°, respectively). The opposite part of the macrocycle is not exactly parallel to the first one, although the atoms that comprise it all lay in one plane and the aromatic character of the compound is confirmed by the bond lengths (Table 2). Similarly to the **4Cu** structure, the lone electron pair of N(5) of the crown ether joins the aromatic system of the macrocycle and, therefore, fixes the location of the crown at the angle with respect to the macrocycle plane. Probably due to the negative charge on C(9), the crown moiety is closer to the macrocycle ring than in **4Cu**, with an angle between the average crown ether plane and the macrocycle of less than 90°. The conformation of the crown is close to that preferable for cation complexation, with only O(5) pointing somewhat outside the ring. The fragment including O(4), C(19) and C(20) atoms proved to be disordered. There are two possible conformations that share nearly the same occupation, designated as A and B. The disorder causes quite large thermal ellipsoids in the structure. The more important bond lengths and angles are reported in Table 2.

The PF_6^- ion does not appear to form close contacts with the complexed Ni^{II} ion or **3Ni** moiety and, not being stabilized in the crystal structure by any well-defined interaction, it seems to rotate freely in the space among the **3Ni** molecules. This may explain the severe disorder in the ion's

Table 2. Important structural parameters for **3Ni** (distances in Å)

Parameter definition	
Ni(1)−N(1)	1.837(3)
Ni(1)−N(3)	1.847(3)
Ni(1)−N(4)	1.851(3)
Ni(1)−N(2)	1.851(3)
C(1)−N(1)	1.472(5)
C(1)−C(2)	1.505(6)
C(2)−N(2)	1.469(5)
C(3)−N(2)	1.277(4)
C(3)−C(4)	1.419(5)
C(4)−C(12)	1.401(5)
C(4)−C(5)	1.422(5)
C(5)−N(3)	1.292(5)
C(6)−N(3)	1.476(4)
C(6)−C(7)	1.489(5)
C(7)−N(4)	1.477(5)
C(8)−N(4)	1.297(5)
C(8)−C(9)	1.396(6)
C(9)−C(10)	1.394(6)
C(9)−C(11)	1.427(6)
C(10)−N(1)	1.293(5)
C(11)−O(1)	1.215(5)
C(12)−N(5)	1.305(5)
C(13)−N(5)	1.466(5)
C(18)−O(4B)	1.27(2)
C(18)−O(4A)	1.56(1)
C(19A)−O(4A)	1.392(9)
C(19A)−C(20A)	1.43(2)
C(20A)−O(5)	1.44(2)
C(19B)−O(4B)	1.28(2)
C(19B)−C(20B)	1.56(3)
C(20B)−O(5)	1.42(2)
C(22)−N(5)	1.463(5)
Average interatomic distances in the crown ether	
C−C	1.48(1)
C−O	1.42(1)
Average P−F bond length	
P−F	1.49(4)

structure. At least four possible conformations for the ion may appear.

The packing of the **3Ni** and PF_6^- ions resembles that observed in **4Cu**. Again, there are two different layers, one consisting of the parallel placed macrocycle moieties and another built up by the crown ethers, forming cages of each pair of crown moieties (Figure 4). The PF_6^- ions are located in tunnels formed in bends of the **3Ni** moieties. Again, there are no significant interactions such as hydrogen bond that would stabilize the structure.

Electrochemical Characteristics of Cu and Ni Complexes

Cyclic voltammograms (CV) of the studied complexes recorded in ACN containing 0.1 M $[Bu_4N]BF_4$ are presented in Figure 5. The CV of complexes **2Cu** and **4Cu** exhibit two reversible redox couples, $Cu^{II/I}$ and $Cu^{II/III}$, respectively. Comparison of the corresponding E_fs (Table 3) indicates that the aza crowns facilitate the $Cu^{II/III}$ redox process and

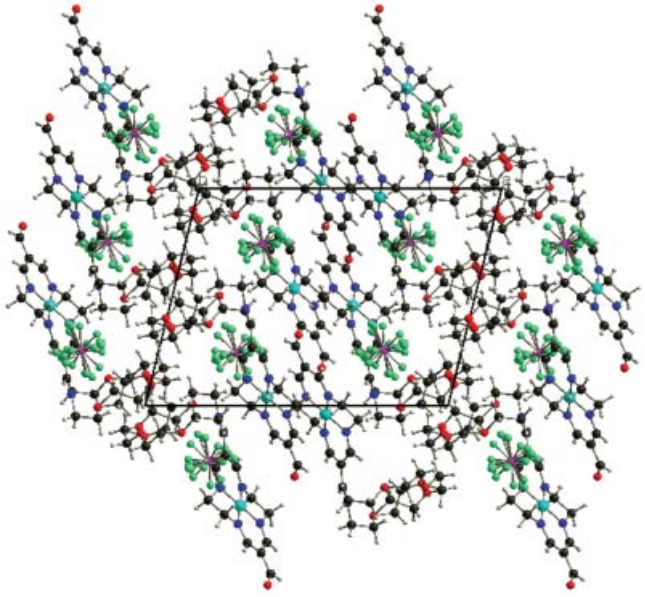

Figure 4. Packing of **3Ni** molecules in the crystal lattice − view along the *y*-axis

make the $Cu^{II/I}$ process more difficult. **3Ni** exhibits a reversible $Ni^{II/III}$ redox process, similar to complex **4Ni**, and an irreversible $Ni^{II/I}$ process.

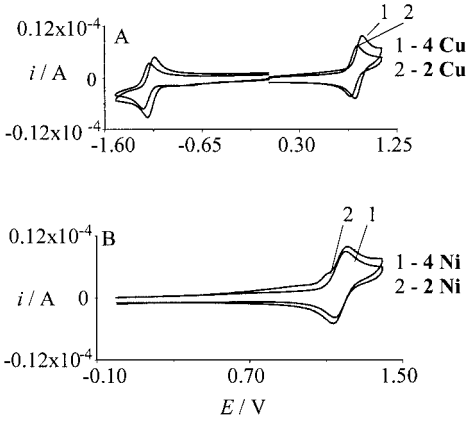

Figure 5. Cyclic voltammograms of the studied complexes (5×10^{-4} M): (A) 1 − **4Cu**, 2 − **2Cu**; (B) 1 − **4Ni**, 2 − **2Ni**

Table 3. Formal potentials of $Cu^{II/I}$, $Cu^{II/III}$ and $Ni^{II/III}$ redox couples in Cu and Ni complexes

Complex	E_f [V] vs. MCE M^{II}/M^{I}	E_f [V] vs. MCE M^{II}/M^{III}
2Cu	−1.150	0.880
2Ni	−1.510[a]	1.179
3Ni	−1.700[a]	1.000
4Cu	−1.200	0.830
4Ni	−1.590[a]	1.170

[a] Potential of irreversible cathodic peak.

Complexation of Cations

The addition of increasing amounts of Li^+ and Na^+ cations to a solution of **3Ni** resulted in a weak positive poten-

Table 4. Shifts of the formal potential of $Ni^{II/III}$ in complex **3Ni** upon addition of metal cations

	Na^+ (1 equiv.)	Li^+ (1 equiv.)	K^+ (1 equiv.)	Mg^{2+} (0.25 equiv.)	Ba^{2+} (0.25 equiv.)	Mg^{2+} (0.5 equiv.)	Ba^{2+} (5 equiv.)
ΔE/mV	10	5	–	10	6	E_a/V = 1.21[a]	E_a/V = 1.21[a]
ΔE/mV	−28	−18	−5	E_c/V = −1.50[b]	E_c/V = −1.70	E_c/V = −1.50	

[a] New anodic peak. [b] New cathodic peak.

tial shift of the $Ni^{II/III}$ redox couple and a more pronounced anodic shift of the $Ni^{II/I}$ cathodic wave (Table 4). With further addition of Li^+ and Na^+ cations the $Ni^{II/III}$ redox potential did not change; however, the $Ni^{II/I}$ potential shifted by 70 mV and by about 100 mV in the presence of 10 equiv. of Li^+ and Na^+, respectively. These results indicate that the binding ability of Li^+ and Na^+ cations to the crown ether moiety is significant when Ni^{II} in the azamacrocycle is reduced to Ni^{I}. With Ni^{III} the complexation of both cations is very weak. The addition of K^+ did not change the $Ni^{II/III}$ potential, and changed only slightly (5 mV) the $Ni^{II/I}$ potential.

The addition of 0.25 equiv. of Mg^{2+} cation to the solution of **3Ni** resulted in an anodic shift of the $Ni^{II/III}$ redox potential by 10 mV and the appearance of a new irreversible $Ni^{II/I}$ peak at the potential 200 mV less negative (Table 4). After addition of 0.5 equiv. of Mg^{2+} a new anodic peak *a* appeared at 170 mV more positive (see A in Figure 6). With increasing Mg^{2+} the current of the new anodic peak increased at the expense of the anodic current of the original peak. At higher concentrations of Mg^{2+} two peaks could be still observed on the differential pulse voltammograms. The currents of both peaks vs. the equivalents of Mg^{2+} added are plotted in Figure 7. However, the reduction current corresponding to the first process remained unchanged. In the cathodic region, with increasing Mg^{2+} the height of the new peak at −1.500 V increased at the expense of the original peak

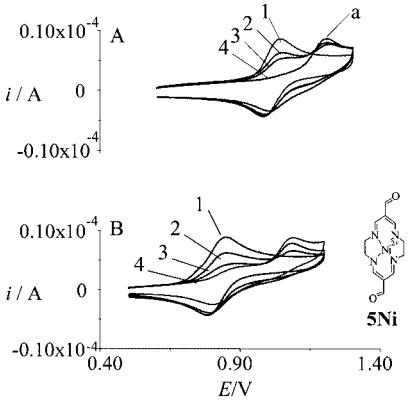

Figure 6. Cyclic voltammograms of 5×10^{-4} M of complexes **3Ni** (A) and **5Ni** (B) upon addition of Mg^{2+} (equiv.): (1) 0; (2) 0.5; (3) 1; (4) 2; inset: structure of **5Ni**

The above effects are explained in Scheme 2.

The small anodic potential shift of E_f after the addition of 0.25 equiv. of Mg^{2+} indicates complexation of this guest

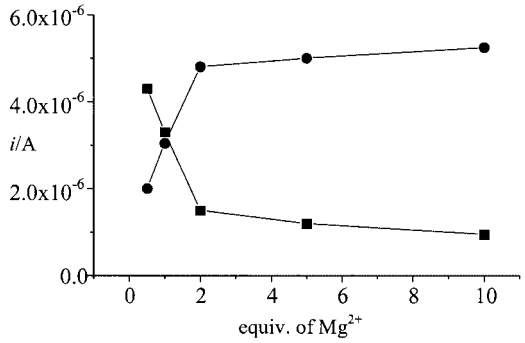

Figure 7. Currents corresponding to the oxidation of Ni^{II} from the aldehyde form of **3Ni** (squares) and from the enolate form (circles) vs. Mg^{2+} added (equiv.)

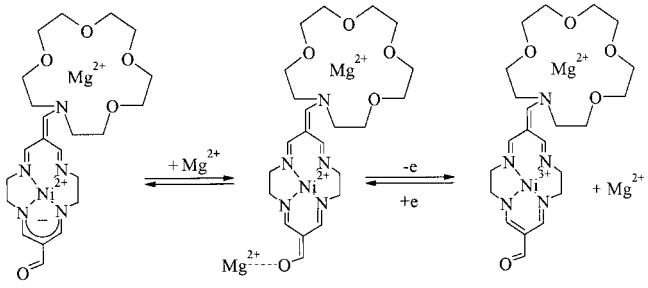

Scheme 2

cation in the crown ether moiety. Further addition of Mg^{2+} forces the charge to shift from the macrocyclic ring to the oxygen of the aldehyde group. This results in the formation of an enolate anion, which interacts with a second Mg^{2+} cation. The second anodic peak corresponds to the oxidation of Ni^{II} from this complex. The so-produced Ni^{III} forces the negative charge to shift again to the macrocyclic ring, with formation of the original complex, which is reduced at about 0.985 V.

To verify the above explanation complex **5Ni** was synthesized.[23] After the addition of Mg^{2+} its electrochemical behavior (Figure 6, B) was similar to that of the **3Ni**. Interaction of an enolate anion with Mg^{2+} was also confirmed by UV/Vis spectroscopy (Figure 8). For both complexes, the absorption band corresponding to Ni^{II} shifts to shorter wavelengths with increasing equivalents of Mg^{2+} cations.

After the addition of 0.25 equiv. of Ba^{2+} the $Ni^{II/III}$ redox potential is shifted towards positive values by 6 mV; however, the second anodic peak at 1.21 V began to appear after the addition of 5 equiv. and increased with the addition of further amounts of Ba^{2+}.

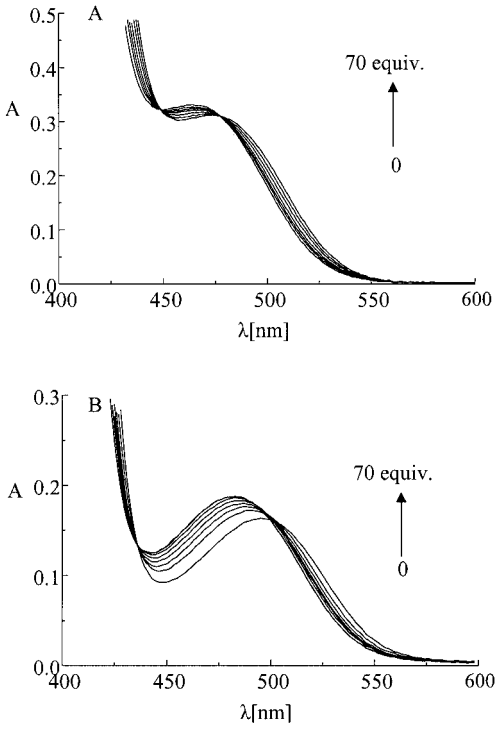

Figure 8. Spectrophotometric titration curves of solutions of **3Ni** (A) and of **5Ni** (B) with $Mg(ClO_4)_2$

The addition of alkali and alkaline earth metal cations to solutions of **4Cu** and **4Ni** had no influence on the E_fs of $Cu^{II/III}$ and $Ni^{II/III}$ redox systems. However, the presence of NH_4^+ exerted a significant influence on the $Cu^{II/I}$ redox process in complex **4Cu**. Figure 9, A, shows the CV of **4Cu** after the addition of 1 equiv. of NH_4^+ cation. The reduction peak *a* at about 200 mV less negative than that of peak *b*, corresponding to the reduction of $Cu^{II/I}$ from complex **4Cu**, is due to the $Cu^{II/I}$ reduction from the part of complex **4Cu** with NH_4^+ cation complexed in the crown ether moiety.

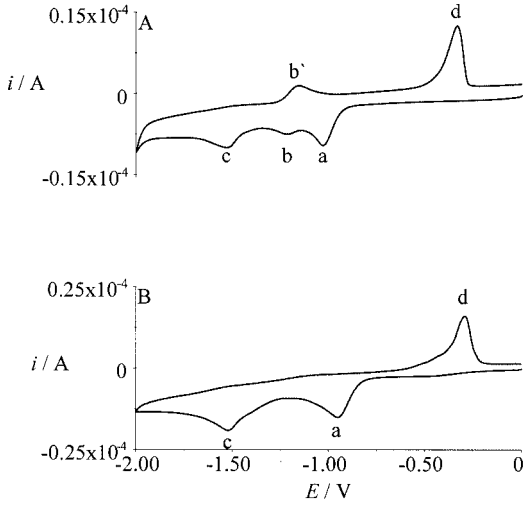

Figure 9. Cyclic voltammograms of complex **4Cu** (5×10^{-4} M) upon addition of (A) 1 equiv. of NH_4^+ and (B) 1 equiv. of Mg^{2+}; scan rate 0.05 Vs^{-1}

Peak *c*, at ca. −1.520 V, corresponds to the $Cu^{I/0}$ reduction in this complex. The proximity of the positively charged cation to the positive copper center can destabilize the complex (which is usually less stable in the case of Cu^+). The anodic peak *d* at ca. −0.300 V corresponds to the oxidation of copper deposited on the electrode surface (which was confirmed by the experiment with CuCl). Peaks *bb′* correspond to the reversible $Cu^{II/I}$ redox process from the original **4Cu** complex. They disappeared at higher concentrations of NH_4^+.

The addition of Na^+ cation had no influence on the $Cu^{II/I}$ redox potential in complex **4Cu**; however, the irreversible $Ni^{II/I}$ potential in complex **4Ni** is shifted anodically by 25 mV after the addition of 20 equiv. of this cation, suggesting that after formation of Ni^I the Na^+ cation is complexed in the crown ether moiety of complex **4Ni**. After the addition of Mg^{2+} cations to the solution of **4Cu** (Figure 9, B) the $Cu^{II/I}$ reduction peak is shifted anodically by about 280 mV (Figure 9, B; peak *a*) versus the original peak *b*. Peaks *c* and *d* were also recorded. A significant increase in both reduction currents (peaks *a* and *c*) indicates that the proximity of Mg^{2+} in the crown ether moiety to the positive copper center can destabilize the complex on the level of Cu^{II}. Such behavior may also be connected with a relatively high concentration of Mg^{2+} in the double layer region. In such a case, Mg^{2+} may influence the electrochemical behavior of the copper center in the azamacrocycle. The CV curves of complex **4Cu** in the presence of Ca^{2+} were similar.

Recognition of Amino Acids

The two α-amino acids (leucine and glycine), β-alanine and lysine (Scheme 3) were chosen as substrate molecules that might interact with complexes **4Cu** and **4 Ni**. Leucine and glycine may interact only with the crown ether moiety (NH_3^+ group) or with the metal cation in the macrocyclic ring through the formation of a coordination bond with the COO^- group. β-Alanine and, especially, lysine, due to the carboxylic and NH_3^+ groups at C-ω, are expected to undergo two-centered fixation. Studies were carried out in acetonitrile/water, 4:1, due to the insolubility of amino acids in pure aprotic solvent.

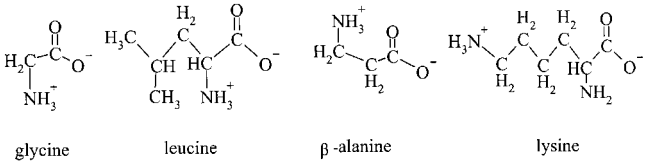

Scheme 3

Unfortunately, electrospray ionization mass spectrometry revealed the decomposition of complexes **4Cu** and **4Ni** (more rapidly) in the presence of leucine and lysine. The peak at *m/z* = 220.2 (Figure 10) corresponds to the free, protonated aza crown ether. The decomposition rate in the presence of lysine (pH of the medium 9.3) was faster than in the presence of leucine (pH of the medium 6.2). Therefore, electrochemical measurements were carried over a short time (3 min after addition of amino acids). Figure 11 shows

the differential pulse voltammogram (DPV) of the **4Cu** complex recorded after the addition of 2 equiv. of leucine or lysine. In both cases the $Cu^{II/III}$ redox peak diminishes and starts to be irreversible. In the presence of leucine, the $Cu^{II/III}$ peak potential is shifted cathodically by 7 mV, and in the presence of lysine by 40 mV. A potential shift of 10 mV was observed after the addition of 2 equiv. of glycine, and of 30 mV after addition of 2 equiv. of β-alanine. A slight cathodic potential shift with leucine and glycine may be due to the interaction of Cu^{III} with the carboxylic group. The presence of the positively charged NH_3^+ group in the immediate vicinity of the COO^- group and of a highly charged Cu^{III} ion may explain the small potential shift and destabilization of the Cu^{III} complex. The more substantial potential shift observed for β-alanine is consistent with a stronger interaction of the carboxylic group with the Cu^{III} center due to the presence of the charged ammonium group at C-β. For lysine, one can expect the two-center interactions − of the carboxylic group with the Cu^{III} center and of the NH_3^+ group at C-ω with the crown ether moiety. In this case the potential shift (40 mV) may be the result of these two effects − the cathodic shift due to the coordination of the carboxylic group, and the anodic potential shift due to complexation of the charged ammonium group. We found that after the addition of 2 equiv. of acetate anion to a solution of complex **6Cu**[24] (Scheme 4) the $Cu^{II/III}$ potential shifted 80 mV towards less positive values.

Crystallographic data indicate that the lone-pair electrons of the crown ether nitrogen atom contribute to the electron density of the cyclidene macrocycle. This may diminish the binding properties of the crown ether moiety towards cat-

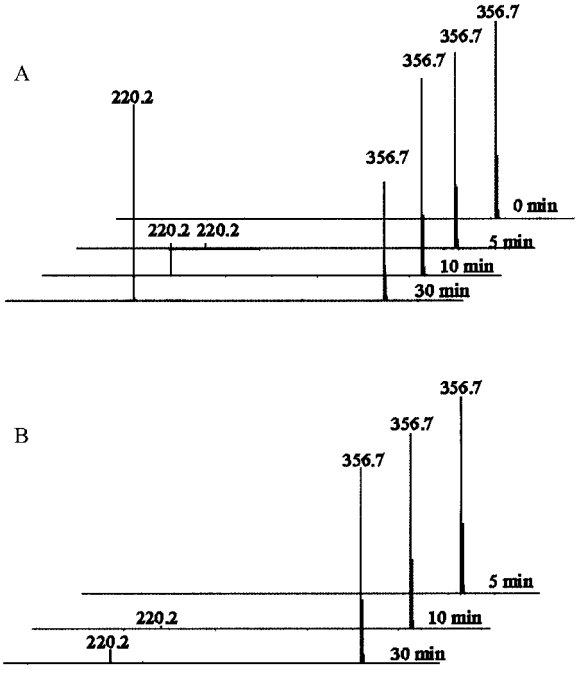

Figure 10. Electrospray ionization mass spectra as a function of time in acetonitrile/H_2O, 4:1, solutions containing 10^{-5} M of complex **4Cu** + 10^{-4} M of the corresponding amino acid: (A) lysine and (B) leucine

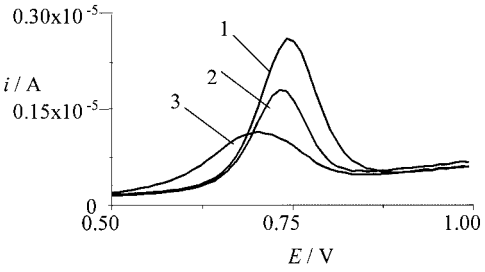

Figure 11. Differential pulse voltammograms of complex **4Cu** recorded in acetonitrile/H_2O, 4:1, containing 0.1 M $[Bu_4N]BF_4$ as supporting electrolyte: (1) 5×10^{-4} M **4Cu**, (2) with 2 equiv. of leucine, and (3) with 2 equiv. of lysine

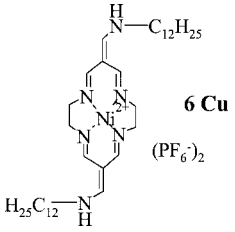

Scheme 4

ions. Conversely, the interaction of the carboxylic group with the central copper ion should reverse this effect and facilitate complexation of the ammonium group in the presence of lysine. Simultaneous binding of carboxylic and ammonium groups with leucine is not possible due to the short distance between them.

Conclusion

Comparison of the E_fs for complexes **4Cu** and **2Cu** indicates that the presence of aza crowns facilitates the $Cu^{II/III}$ redox process and makes the $Cu^{II/I}$ process more difficult.

The interaction of Na^+ and Li^+ with the **3Ni** complex was quite weak. In the presence of Mg^{2+}, the ligand aldehyde isomerizes to enolate ion. Crystallographic data indicate that the lone-pair electrons on the crown ether nitrogen atom contribute to the electron density of the cyclidene macrocycle. This may be one of the reasons why the addition of alkali and alkaline earth metal cations to the solutions of **4Cu** and **4Ni** has no influence on the E_fs of $Cu^{II/III}$ and $Ni^{II/III}$ redox systems. However, the presence of NH_4^+, Mg^{2+} and Ca^{2+} cations influences significantly the $Cu^{II/I}$ redox process in complex **4Cu**.

A more pronounced shift of the $Cu^{II/III}$ potential in **4Cu** in the presence of lysine than with leucine suggests that there is, in the first case, a simultaneous interaction between the NH_3^+ group and the crown ether moiety and between the carboxylic group and the Cu^{III} center.

Experimental Section

Chemicals: All solvents (Merck) were used without further purification. Deionized water from a Milli-Q system (Millipore, Bedford,

MA, USA), distilled additionally from a quartz still, was used. As supporting electrolyte, electrochemical grade $[Bu_4N]BF_4$ (Fluka) was used. Cations were added as their perchlorate salts.

Instrumentation: Cyclic and differential pulse voltammograms were measured at a glassy carbon (GC-20) electrode with a Pt plate as the counter electrode and an Ag/Ag^+ reference electrode. This was connected to the electrolytic cell via an intermediate vessel filled with the solution under investigation. The Ag/Ag^+ reference electrode contained an internal solution of 0.001 M $AgNO_3$ + 0.10 M $[Bu_4N]BF_4$ in acetonitrile. The potential of this reference electrode was 200 mV vs. 1 M NaCl aqueous calomel electrode (MCE). All potentials in this paper are expressed vs. this reference electrode. Solutions were deaerated by flushing with pure argon. The measuring system was an Autolab (EcoChemie, Netherlands). Electronic spectra were recorded using a Cary 1 (Varian) spectrophotometer. NMR spectra were obtained on a Varian Mercury 400 spectrometer. Signals are reported in ppm relative to residual solvent signal. IR spectra (paraffin oil mulls) were recorded with a Perkin−Elmer Spectrum 2000 FT-IR spectrometer. ESI mass spectra were measured on a Mariner Perseptive Biosystem mass spectrometer.

Synthesis

Syntheses of 5,12-dimethyl-1,4,8,11-tetraazacyclotetradeca-4,11-diene diperchlorate and of complexes **1Cu** and **1Ni** have been described elsewhere.[24]

[6,13-Bis(morpholinomethylidene)-1,4,8,11-tetrazacyclotetradeca-4,7,11,14-tetraene]nickel(II) Bis(hexafluorophosphate) (2Ni): Morpholine (0.18 cm^3, 1 mmol) was added to a solution of complex **1Ni** (0.32 g, 0.5 mmol) in dry acetonitrile (25 mL). The mixture was then stirred for 4 h at room temperature, and the resulting solution was applied to a 2 × 20 cm acidic alumina column. The column was then washed with acetonitrile. A fast-moving orange band was collected, evaporated and dissolved in acetonitrile/H_2O, 1:1. Solid NH_4PF_6 (0.2 g) was then added to the solution and the resultant orange crystalline product that precipitated upon evaporation of acetonitrile was filtered off and dried under reduced pressure. Yield 0.29 g, 79%. $C_{20}H_{30}N_6NiO_2{\cdot}(PF_6)_2$ (735.1): calcd. C 32.7, H 4.1, N 11.4; found C 32.9, H 4.1, N 11.4. ^1H NMR (CD_3CN, 400 MHz): δ = 3.54 (s, 8 H, NCH_2CH_2N), 3.69 (b. m, 4 H, morpholine CH_2 groups), 3.70 (b. m, 4 H, morpholine CH_2 groups), 3.82 (b. m, 8 H, morpholine CH_2 groups), 7.58 (s, 2 H, exoc. =CH−N), 7.74 (b. s, 4 H, N=C−H). ^{13}C NMR (CD_3CN, 100 MHz): 51.7, 57.1, 66.1 and 67.2 (morpholine CH_2), 60.1 (b, NCH_2CH_2N), 103.6 (ring-C=), 162.9 (exoc. =CH−N, ring H−C=N signals were not observed due to dynamic line broadening). IR (Nujol): $\tilde{\nu}$ = 1600 and 1568 (ν C=N and C=C), 840 and 558 (PF_6^-) cm^{-1}. UV/Vis (CH_3CN, nm): λ_{max} (ε) = 267 (28980), 380 (52360), 459 (1400). ESI MS: *m*/*z* = 444.2 $[C_{20}H_{30}N_6NiO_2]^{2+}$.

[6,13-Bis(morpholinomethylidene)-1,4,8,11-tetraazacyclotetradeca-4,7,11,14-tetraene]copper(II) Bis(hexafluorophosphate) (2Cu): Complex was synthesized from copper(II) complex **1Cu** following the same procedure as for **2Ni**. Yield 75%. $C_{20}H_{30}CuN_6O_2{\cdot}(PF_6)_2$ (740.0): calcd. C 32.5, H 4.1, N 11.4; found C 32.6, H 4.2, N 11.5. IR (Nujol): $\tilde{\nu}$ = 1599 (ν C=N and C=C), 833 and 533 (PF_6^-) cm^{-1}. UV/Vis (CH_3CN, nm): λ_{max} (ε) = 294 (27370), 347 (65900), 507 (301). ESI MS: *m*/*z* = 224.6 $[C_{20}H_{30}CuN_6O_2]^{2+}$.

{6,13-Bis[(1,4,7,10-tetraoxa-13-azacyclooctadecano-13-yl)methylidene]-1,4,8,11-tetraazacyclotetradeca-4,7,11,14-tetraene}nickel(II) Bis(hexafluorophosphate) (4Ni): 1,4,7,10-Tetraoxa-13-azacyclooctadecane (0.22 g, 1 mmol) was added to a solution of complex **1Ni** (0.315 g, 0.5 mmol) in dry acetonitrile (25 mL). The mixture was then stirred for 4 h at room temperature, and the resulting solution was applied to a 2 × 20 cm acidic alumina column. The column was subsequently washed with acetonitrile. A fast-moving orange band was then collected, evaporated and crystallized from acetonitrile/water. The orange crystalline product that precipitated upon evaporation of acetonitrile was filtered off and dried under reduced pressure. Yield 0.39 g, 78%. $C_{32}H_{54}N_6NiO_8{\cdot}(PF_6)_2$ (999.4): calcd. C 38.5, H 5.5, N 8.4; found C 38.4, H 5.5, N 8.5. ^1H NMR (CD_3CN, 400 MHz): δ = 3.60−3.90(m, 48 H, NCH_2CH_2N and crown ether CH_2 groups), 7.66 (s, 2 H, exocyclic =CH−N), 7.99 (v.b. s, 4 H, ring N=C−H). ^{13}C NMR (CD_3CN, 100 MHz): 55.7, 61.6, 68.0, 69.8, 70.7, 70.8, 70.9, 71.1, 71.2, 71.3 (crown ether CH_2), 60.1 (broad, ring NCH_2-CH_2N), 104.7 (ring =C; ring H−C=N signals were not observed due to dynamic line broadening), 165.3 (exocyclic = CH−N). IR (Nujol): $\tilde{\nu}$ = 1594 vs, 1559 w (ν C=N and C=C), 842 vs and 559 s (PF_6^-) cm^{-1}. UV/Vis (CH_3CN): λ_{max} (ε) = 267 (28980), 380 (52360), 459 (1400) nm. ESI MS (CH_3CN, *m*/*z*): 354.2$[C_{32}H_{54}O_8N_6Ni]^{2+}$.

{6-Formyl-13-[(1,4,7,10-tetraoxa-13-azacyclooctadecano-13-yl)methylidene]-1,4,8,11-tetraazacyclotetradeca-4,7,11,14-tetraen}-nickel(II) Hexafluorophosphate (3Ni): 1,4,7,10-Tetraoxa-13-azacyclooctadecane (0.11 g, 0.5 mmol) was added to a solution of complex **1Ni** (0.315 g, 0.5 mmol) in dry acetonitrile (25 mL). The mixture was then stirred for 2 h at room temperature. The resulting solution was diluted with water (25 mL) and applied to the SP Sephadex C25 cation exchange column (25 × 2 cm). The column was then washed with water and eluted with 0.2 M Na_2SO_4 solution. Two resultant orange bands were separated and the products precipitated with an excess NH_4PF_6. After filtration the isolated solid products were dissolved in acetonitrile, diluted with water/ethanol, 1:1, and crystallized upon slow evaporation of solvents. The first fraction contained complex **3Ni** (yield 30%), and the previously described complex **4Ni** was isolated from the second fraction. $C_{22}H_{34}N_5NiO_5{\cdot}PF_6$ (652.2): calcd. C 40.5, H 5.3, N 10.7; found C 40.4, H 5.3, N 10.5. ^1H NMR (CD_3CN, 400 MHz): δ = 3.60−3.90 (m, 28 H, NCH_2CH_2N and crown ether CH_2 groups), 7.57 (s, 1 H, exocyclic =CH−N), 7.50 (v.b. s, 1 H) and 8.37 (v.b. s, 1 H, ring N=C−H crown ether site), 7.50 (b. s, 1 H) and 7.86 (b. s, 1 H, ring N=C−H formyl site), 9.20 (s, 1 H, O=C−H). ^{13}C NMR (CD_3CN, 100 MHz): δ = 55.5, 61.5, 68.2, 70.0, 70.7, 70.8, 71.0, 71.2, 71.2, 71.2 (crown ether CH_2), 58.6, 59.0, 59.3, 60.8 (broad, ring NCH_2-CH_2N), 104.8 (ring =C−CHN), 114.2 (ring =C−CHO, ring H−C=N not observed), 164.5 (=CH−N), 187.3 C=O. IR (Nujol): $\tilde{\nu}$ = 1656 m,1594 vs, 1569 m, 1541 (ν C=O, C=N and C=C), 841 vs and 558 s (PF_6^-) cm^{-1}. UV/Vis (CH_3CN, nm): λ_{max} (ε) = 247 (15900), 281 (26880), 357 (28140), 371 (29040), 474 sh (636). ESI MS (CH_3CN): *m*/*z* = 506.2 $[C_{22}H_{34}N_5NiO_5]^+$.

{6,13-Bis[(1,4,7,10-tetraoxa-13-azacyclooctadecano-13-yl)methylidene]1,4,8,11-tetraazacyclotetradeca-4,7,11,14-tetraene}copper(II) Hexafluorophosphate (4Cu): This complex was synthesized from copper(II) complex **1Cu** following the same procedure as with **4Ni**. Yield 85%, red crystals. $C_{32}H_{54}CuN_6O_8{\cdot}(PF_6)_2$ (1004.3): calcd. C 38.3, H 5.4, N 8.4; found C 38.3, H 5.5, N 8.5. IR (Nujol): $\tilde{\nu}$ = 1646 w, 1599 s, 1587 s (PF_6^-), 841 vs and 558 s (PF_6^-) cm^{-1}. UV/Vis (CH_3CN, nm): λ_{max} (ε) = 290 (17050), 345 (43050), 492 (306). ESI MS (CH_3CN) *m*/*z* =356.7 $[C_{32}H_{54}CuN_6O_8]^{2+}$.

X-ray Crystallographic Study: The structures of **3Ni** and **4Cu** complexes were determined in single-crystal X-ray diffraction experiments. Both measurements were performed on a Kuma KM4CCD κ-axis diffractometer with graphite-monochromated Mo-K_α radi-

ation (λ = 0.71073 A, 45.0 kV, 40.0 mA) at room temperature (293 K). In each experiment the crystal was positioned 62 mm from the KM4CCD camera. Some 600 frames were measured for each crystal at 1.0° intervals with counting times of 33 s for the **3Ni** crystal and 27 s for **4Cu**. A numeric absorption correction was applied to the collected datasets. Data reduction and analysis were carried out with the Kuma Diffraction programs.

The structures were solved by direct methods using the SHELXS-97[25] program and subsequent refinement was also carried out with SHELXL-97.[26] Refinement was based on F^2 for all reflections except those with negative intensities. Weighted R factors, wR and all goodness-of-fit S values were based on F^2, whereas conventional R factors were based on the amplitudes, with F set to zero for negative F^2. The $F_o^2 > 2\sigma(F_o^2)$ criterion was applied only in calculating R factors and was not relevant to the choice of reflections for the refinement. The R factors based on F^2 are, for both structures, about twice as large as those based on F. For the **3Ni** structure some hydrogen atoms were located in idealized geometrical positions. Also, some special constraints were applied to the anisotropic displacement parameters of some atoms; the constraints were necessary due to disorder in the crown-ether compound and PF_6^- ion. Scattering factors were taken from Table 4.2.6.8 and 6.1.1.4 of International Crystallographic Tables Vol. C.[27]

3Ni: $C_{22}H_{34}NiN_5O_5{\cdot}PF_6$, M = 652.22, T = 293(2) K, λ = 0.71073 Å; crystal system, monoclinic; space group, $P2_1/c$; unit cell dimensions, a = 18.454(4) Å, b = 11.406(2) Å, c = 13.642(3) Å, α = 90°, β = 103.93(3)°, γ = 90°; V = 2787.0(10) Å^3; Z = 4; calculated density = 1.554 Mg m^{-3}; absorption coefficient = 0.836 mm^{-1}; F(000) = 1352; crystal size: 0.34 × 0.16 × 0.07 mm; θ range for data collection: 3.41 to 22.50°; index range: $-19 \le h \le 19$, $-12 \le k \le 12$, $-12 \le l \le 14$; reflections collected = 16239; unique reflections = 3637 [R_{int}= 0.0632]; completeness to θ = 22.50°: 99.7%; refinement method, full-matrix least-squares on F^2, data/restraints/parameters: 3637/51/460; goodness-of-fit on F^2 = 1.148; final R int [$I > 2\sigma(I)$]: $R1$ = 0.0445, $wR2$ = 0.1170; R int (all data): $R1$ = 0.0589, $wR2$ = 0.1273; extinction coefficient = 0.0020(7); weight = $1/[\sigma^2(F_o^2) + (0.0712P)^2 + 0.00P]$ where $P = [\max(F_o^2, 0) + 2F_c^2]/3$; largest diffraction peak and hole: 0.604 and −0.348 e·Å^{-3}.

4Cu: $C_{32}H_{54}CuF_{12}N_6O_8P_2$, M = 1004.29, T = 293 K, λ = 0.71073 Å; crystal system, triclinic; space group, $P\bar{1}$; unit cell dimensions, a = 8.7793(18) Å, b = 9.783(2) Å, c = 13.301(3) Å, α = 106.50(3)°, β = 103.90(3)°, γ = 93.88(3)°; V = 1051.9(4) Å^3; Z = 1; calculated density = 1.585 Mg m^{-3}; absorption coefficient = 0.703 mm^{-1}, F(000) = 51, crystal size = 0.30 × 0.20 × 0.10 mm, θ range for data collection = 3.32 to 22.50°; index ranges: $-8 \le h \le 9$, $-10 \le k \le 10$, $-14 \le l \le 14$; reflections collected = 6301, unique reflections = 2740 [R_{int} = 0.0443]; completeness to θ = 22.50°: 99.5%; refinement method, full-matrix least-squares on F^2; data/restraints/parameters: 2740/0/386; goodness-of-fit on F^2 = 1.056; final Rint [$I > 2\sigma(I)$]: $R1$ = 0.0374, $wR2$ = 0.0989; R int (all data): $R1$ = 0.0437, $wR2$ = 0.1047; extinction coefficient = 0.004(2); weight = $1/[\sigma^2(F_o^2) + (0.0671P)^2 + 0.2486P]$ where $P = [\max(F_o^2, 0) + 2F_c^2]/3$; largest diffraction peak and hole: 0.413 and −0.287 e·Å^{-3}.

CCDC-227140 and -227141 (for **3Ni** and **4Cu**, respectively) contain the supplementary crystallographic data for this paper. These data can be obtained free of charge at www.ccdc.cam.ac.uk/conts/retrieving.html [or from the Cambridge Crystallographic Data Centre, 12 Union Road, Cambridge CB2 1EZ, UK; Fax: (internat.) +44-1223-336-033; E-mail: deposit@ccdc.cam.ac.uk].

Acknowledgments

Financial support for B. K. D. and K. W. by the State Committee for Scientific Research (project 4 T09A 048 23) is gratefully acknowledged. The authors are grateful to Mrs. S. Pawłowska for technical help. X-ray measurements were undertaken in the Crystallographic Unit of the Physical Chemistry Laboratory at the Chemistry Department of the University of Warsaw.

[1] P. D. Beer, *Adv. Inorg. Chem.* **1992**, *39*, 79−154.
[2] P. D. Beer, P. A. Gale, Z. Chen, *Adv. Phys. Org. Chem.* **1998**, *31*, 1−84.
[3] P. D. Beer, P. A. Gale, G. Z. Chen, *Coord. Chem. Rev.* **1999**, 185−186, 3−36.
[4] P. L. Boulas, M. Gómez-Kaifer, L. Echengoyen, *Angew. Chem. Int. Ed.* **1998**, *37*, 216−247.
[5] I. Ion, J. C. Moutet, A. Popescu, E. Saint-Aman, L. Tomazeswski, I. Gautier-Luneau, *J. Electroanal. Chem.* **1997**, *440*, 145−152.
[6] H. Plenio, D. Burth, *Organometallics* **1996**, *15*, 4054−4062.
[7] C. D. Hall, S. Y. Chu, *J. Organomet. Chem.* **1995**, *498*, 221−228.
[8] H. Plenio, R. Diodone, *J. Organomet. Chem.* **1995**, *492*, 73−80.
[9] H. Plenio, C. Aberle, *Organometallics* **1997**, *16*, 5950−5957.
[10] H. Plenio, J. Yang, R. Diodone, J. Heinze, *Inorg. Chem.* **1994**, *33*, 4098−4104.
[11] J. C. Medina, T. T. Goodnow, S. Bott, J. L. Atwood, A. E. Kaifer, G. W. Gokel, *J. Chem. Soc., Chem. Commun.* **1991**, 290−292.
[12] V. Balzani, M. Gómez-López, J. F. Stoddart, *Acc. Chem. Res.* **1998**, *31*, 405−416.
[13] A. P. de Silva, H. Q. N. Gunarante, C. P. McCoy, *Nature* **1993**, *346*, 42−44.
[14] E. V. Rybak-Akimova, Y. D. Lampeka, *Supramol. Chem.* **1995**, *4*, 297−304.
[15] O. P. Kryatova, A. G. Kolchinski, E. V. Rybak-Akimova, *Tetrahedron* **2003**, *59*, 231−239.
[16] O. P. Kryatova, A. G. Kolchinski, E. V. Rybak-Akimova, *J. Inclus. Phenom.* **2002**, *42*, 251−260.
[17] P. V. Bernhardt, E. J. Hayes, *Inorg. Chem.* **2002**, *41*, 2892−2902.
[18] L. Fabbrizzi, M. Licchelli, P. Pallavicini, *Acc. Chem. Res.* **1999**, *32*, 846−853.
[19] J. Taraszewska, K. Zięba, B. Korybut-Daszkiewicz, *Electrochim. Acta* **2001**, *46*, 3219−3225.
[20] V. Thanabal, V. Krishnan, *J. Am. Chem. Soc.* **1982**, *104*, 3643−3650.
[21] O. E. Sielcken, M. M. Tilborg, M. F. M. Roks, R. Hendriks, W. Drenth, R. J. M. Nolte, *J. Am. Chem. Soc.* **1987**, *109*, 4261−4265.
[22] E. Kimura, H. Fujioka, M. Kodama, *J. Chem. Soc., Chem. Commun.* **1986**, 1158−1159.
[23] W. Grochala, A. Jagielska, K. Woźniak, A. Więckowska, R. Bilewicz, B. Korybut-Daszkiewicz, J. Bukowska, L. Piela, *J. Phys. Org. Chem.* **2001**, *14*, 63−73.
[24] B. Korybut-Daszkiewicz, A. Więckowska, R. Bilewicz, S. Domagała, K. Woźniak, *J. Am. Chem. Soc.* **2001**, *123*, 9356−9366.
[25] G. M. Sheldrick, *Acta Crystallogr., Sect. A* **1990**, *46*, 467−473.
[26] M. Sheldrick, *SHELXL-97. Program for the Refinement of Crystal Structures; University of Göttingen, Germany.*
[27] *International Tables of Crystallography* (Ed.: A. J. C. Wilson), Kluwer, Dordrecht, **1992**, vol. C, 19.

Received December 9, 2003
Early View Article
Published Online June 11, 2004

